Power Grid Partitioning: Static and Dynamic Approaches

Miao Zhang, Zhixin Miao, Lingling Fan
Department of Electrical Engineering
University of South Florida
Tampa FL 33620
miaozhang@mail.usf.edu
{zmiao, linglingfan}@usf.edu

***Abstract*—This paper presents three power grid partitioning methods, which are classified into two categories: static and dynamic approaches. In the static approaches, spectral clustering method based on eigenvectors of the graph Laplacian and mixed-integer programming (MIP) strategy have been used to partition a grid. In dynamic approach, slow coherency based on the eigenvector of inter-area oscillation mode is used for generator grouping. We show the three methods lead to the same partitioning results and give the underlying reason.**

***Index Terms*—power system partitioning, spectral clustering, MIP, generator grouping, slow coherency.**

I. Introduction

Power grid clustering strategies in the literature can be classified into two categories: static and dynamic. Static approach concerns only grid topology, connectivity and steady-state characteristics. For example, in [1], the electrical coupling strength is used as a coefficient for the analysis of electrical connection, and the electrical modularity is used to assess the quality of the partition. The objective of [1] is to identify boundaries of virtual microgrids in a radial distribution network. Graph Laplacian based on the admittance matrix of a power grid is used in [2], [3] for grid partitioning. The method is named as spectral clustering where eigenvectors of the graph Laplacian will be used for clustering. A tutorial for spectral clustering algorithm based can be found in [4]. Alternatively, mixed integer programming (MIP) problem is formulated to give an optimal partition solution in [5]. The formulation tries to separate a grid into multiple balancing areas with minimum load shedding.

The dynamic approach mainly deals with the system dynamic matrix. Generators are grouped based on eigenvectors of the dominant inter-area oscillation modes. This method of generator clustering is named as "slow coherence" in [6]. The generators oscillation modes are highly related to the network topology represented by the admittance matrix (Ybus) and generator dynamic properties. This fact is indicated intuitively in [6]. In [7], a quantitative description of the relationship of inter-area oscillation modes and the eigenvalues of coupling graph Laplacian dependent on both topology and power transfer pattern is given. Similar findings have been documented in [8] and [9]. The network Laplacian's eigenvalues determine the grid robustness against lower frequency disturbances, which is revealed in [9].

In this paper, we will conduct the power system partitioning via both static and dynamic approaches. Three methods will be used to partition the IEEE 14-bus system into three areas.

Spectral clustering method clusters buses into three areas. This is a simple and direct way with a given adjacent matrix and the partition number. The spectral clustering method has an objective of minimum number of edges cutting.

MIP partitioning method determines which edges to cut to result in three areas. This method minimizes the total load shedding. The optimization problem has power flow equations as constraints. MIP partitioning has to add the connectivity constraints to guarantee all nodes inside each area are connected. MIP method is more flexible since we can customize the constraints for different purposes. e.g., we can assign the minimum number of nodes for each area and ensure any branch as a boundary branch between two areas.

Finally, the dynamic eigenvector-based clustering method (or slow coherence) is used to cluster generators. The procedure is to build a linear electromechanical (EM) model to find two dominant oscillatory eigenvalues. Based on the corresponding eigenvectors, clustering is conducted.

The major contributions of this paper are as follows. Detailed explanations on three partition methods are given and tested on the IEEE 14-bus system. Methodology similarity of spectral clustering method and slow coherency methods is identified. Both methods rely on eigenvector-based clustering. Further, the reason of similarity of the partitioning results based on spectral clustering and slow coherency is given. Two static methods, spectral clustering and MIP partitioning, are also compared. Reason of the similarity of the partitioning results is given.

This paper is organized as follows. Section II introduces two static approaches: spectral clustering and MIP partitioning. Section III gives the generator grouping approach based on dynamic analysis. IEEE 14-bus system is tested to find the relationship among three approaches. Section IV concludes the paper.

II. Static Approaches

A. Spectral Clustering

In this subsection, the properties of Laplacian's eigenvalues and eigenvectors are introduced first. Then the IEEE 14-bus is tested for three areas clustering via spectral clustering algorithm.

1) Laplacian of Network: Given a power system network $G = (V, E)$ with the bus set V and branch set E.

The Graph Laplacians ($\boldsymbol{L}$) will be built as follows.

$$\boldsymbol{L} = \boldsymbol{D} - \boldsymbol{W} \tag{1}$$

where $\boldsymbol{W}$ is the adjacent matrix and $\boldsymbol{D}$ is a diagonal matrix and its i^{th} diagonal component is notated as d_i where $d_i = \sum_j W_{ij}$. Fig. 1 shows a 6-node graph. It has only 1 connected component, which means it is an entire connected graph. We assume that each item in the adjacent matrix $\boldsymbol{W}$ is defined as

$$w_{i,j} = \begin{cases} 1, & \text{If } i,j \text{ are connected.} \\ 0, & \text{otherwise.} \end{cases} \tag{2}$$

The Laplacian $\boldsymbol{L}$ is:

$$\boldsymbol{L} = \begin{bmatrix} 2 & -1 & -1 & 0 & 0 & 0 \\ -1 & 2 & -1 & 0 & 0 & 0 \\ -1 & -1 & 3 & -1 & 0 & 0 \\ 0 & 0 & -1 & 3 & -1 & -1 \\ 0 & 0 & 0 & -1 & 2 & -1 \\ 0 & 0 & 0 & -1 & -1 & 2 \end{bmatrix}. \tag{3}$$

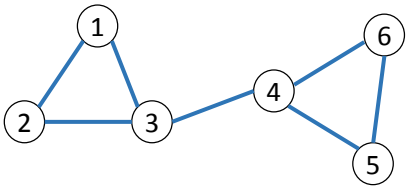

Fig. 1. Connected 6-node graph

2) Eigenvectors Properties: The i^{th} eigenvalue λ_i and eigenvectors $\boldsymbol{v}_i$ have the following relationship (4):

$$\boldsymbol{L}\boldsymbol{v}_i = \lambda_i \boldsymbol{v}_i. \tag{4}$$

In (5), eigenvectors are listed in matrix $\boldsymbol{v}$ by columns. And (6) gives the corresponding eigenvalues: $0 = \lambda_1 \leq \lambda_2 \leq \cdots \leq \lambda_6$.

$$\boldsymbol{v} = \begin{bmatrix} -0.4082 & 0.4647 & -0.1752 & -0.7231 & 0.1724 & -0.1845 \\ -0.4082 & 0.4647 & -0.3438 & 0.6777 & 0.0764 & -0.1845 \\ -0.4082 & 0.2610 & 0.5190 & 0.0454 & -0.2488 & 0.6572 \\ -0.4082 & -0.2610 & 0.5190 & 0.0454 & -0.2488 & -0.6572 \\ -0.4082 & -0.4647 & -0.5575 & -0.1022 & -0.5119 & 0.1845 \\ -0.4082 & -0.4647 & 0.0385 & 0.0568 & 0.7607 & 0.1845 \end{bmatrix} \tag{5}$$

$$\boldsymbol{\lambda} = \begin{bmatrix} 0 & 0.4384 & 3 & 3 & 3 & 4.5616 \end{bmatrix}^T \tag{6}$$

Starting from the second eigenvector $\boldsymbol{v}_2$, which corresponds to the smallest non-zero eigenvalue 0.4384, we assume the element in j-th row i-th column as $x_{i,j}$.

$$x_{i,j} = \begin{cases} 1, & \text{If } v_{i,j} > 0 \\ -1, & \text{If } v_{i,j} < 0 \end{cases} \tag{7}$$

$$\boldsymbol{x} = \begin{bmatrix} \boldsymbol{x}_2 & \boldsymbol{x}_3 & \boldsymbol{x}_4 & \boldsymbol{x}_5 & \boldsymbol{x}_6 \end{bmatrix} = \begin{bmatrix} 1 & -1 & -1 & 1 & -1 \\ 1 & -1 & 1 & 1 & -1 \\ 1 & 1 & 1 & -1 & 1 \\ -1 & 1 & 1 & -1 & -1 \\ -1 & -1 & -1 & -1 & 1 \\ -1 & 1 & 1 & 1 & 1 \end{bmatrix} \tag{8}$$

If we separate this graph into two subareas, then the number of edges being cut based on i^{th} eigenvalue is C_i, which can be computed from $\boldsymbol{x}_i$ based on L:

$$C_i = \frac{1}{4}\boldsymbol{x}_i^T L \boldsymbol{x}_i \tag{9}$$

For example, we can have C_2 and C_3 as

$C_2 = \frac{1}{4}\boldsymbol{x}_2^T \boldsymbol{L}\boldsymbol{x}_2 = 1$, Cut Edge 3-4.

$C_3 = \frac{1}{4}\boldsymbol{x}_3^T \boldsymbol{L}\boldsymbol{x}_3 = 4$, Cut Edges 1-3, 2-3, 4-5, and 5-6.

For the graph in Fig. 1, there is only one zero eigenvalue, since the number of connected components is 1. Its corresponding eigenvector is a scaled vector $\mathbf{1}$ where all elements are the same.

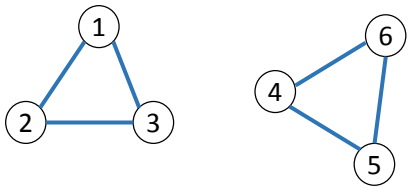

Fig. 2. 2 connected components 6-node graph

If we disconnect Edge 3-4, shown in Fig. 2, we get following eigenvalues and eigenvectors.

$$\boldsymbol{v} = \begin{bmatrix} 0.5774 & 0 & 0.2895 & 0 & 0.7634 & 0 \\ 0.5774 & 0 & 0.5164 & 0 & -0.6325 & 0 \\ 0.5774 & 0 & -0.8059 & 0 & -0.1310 & 0 \\ 0 & 0.5774 & 0 & 0.7634 & 0 & 0.2895 \\ 0 & 0.5774 & 0 & -0.6325 & 0 & 0.5164 \\ 0 & 0.5774 & 0 & -0.1310 & 0 & -0.8059 \end{bmatrix} \tag{10}$$

$$\boldsymbol{\lambda} = \begin{bmatrix} 0 & 0 & 3 & 3 & 3 & 3 \end{bmatrix}^T \tag{11}$$

Note that there are 2 zero eigenvalues in this scenario since there are two connected components in this graph. Also, the corresponding eigenvectors do not consist of identical elements. The Laplacian matrix $\boldsymbol{L}$ has the same number of zero eigenvalues as its connected components.

3) 14-Bus System Partitioning: Based on the properties of graph Laplacian, we know that the number of zero eigenvalues representing the number of connected components. Also, we would like to focus on the small non-zero eigenvalues. The smaller the eigenvalue, the fewer the edges will be cut for partitioning. The spectral clustering method is essentially

clustering based on the eigenvectors of smallest non-zero eigenvalues.

Let us use IEEE 14-bus system for three areas clustering. Generally, the weak connectivity is due to higher impedance transmission lines or fewer connections between two subareas. The admittance matrix $\boldsymbol{Y}$ of a power grid can represent the bus connectivity. If two buses (i and j) are tightly connected, then a large magnitude of Y_{ij} is expected. If they are loosely connected, a small magnitude of Y_{ij} is expected. If they are not connected, then the admittance is zero ($Y_{ij} = 0$).

Hence, we build a graph Laplacian based on the $\boldsymbol{Y}$ matrix. We obtain an adjacent matrix $\boldsymbol{W}$ with its diagonal elements as 0 and non-diagonal elements as the absolute values from the $\boldsymbol{Y}$ matrix:

$$\boldsymbol{W} = \begin{bmatrix} 0 & |Y_{1,2}| & \dots & |Y_{1,n}| \\ |Y_{2,1}| & 0 & \dots & |Y_{2,n}| \\ \vdots & \vdots & \ddots & \vdots \\ |Y_{n,1}| & |Y_{n,2}| & \dots & 0 \end{bmatrix} \tag{12}$$

In (13), we list the first 3 eigenvectors of $\boldsymbol{L}$. The corresponding eigenvalues are given in (14).

$$\boldsymbol{v} = \begin{bmatrix} 0.2673 & 0.3301 & 0.2491 & \dots \\ 0.2673 & 0.3173 & 0.2284 & \dots \\ 0.2673 & 0.3445 & 0.2293 & \dots \\ 0.2673 & 0.2328 & 0.1113 & \dots \\ 0.2673 & 0.2138 & 0.1641 & \dots \\ 0.2673 & -0.2467 & 0.1669 & \dots \\ 0.2673 & 0.1010 & -0.3193 & \dots \\ 0.2673 & 0.1627 & -0.6350 & \dots \\ 0.2673 & -0.0323 & -0.2546 & \dots \\ 0.2673 & -0.1052 & -0.2377 & \dots \\ 0.2673 & -0.2263 & -0.0586 & \dots \\ 0.2673 & -0.4447 & 0.2961 & \dots \\ 0.2673 & -0.3673 & 0.1827 & \dots \\ 0.2673 & -0.2797 & -0.1227 & \dots \end{bmatrix} \tag{13}$$

$$\boldsymbol{\lambda} = \begin{bmatrix} 0 & 2.1531 & 2.8225 & \dots \end{bmatrix}^T \tag{14}$$

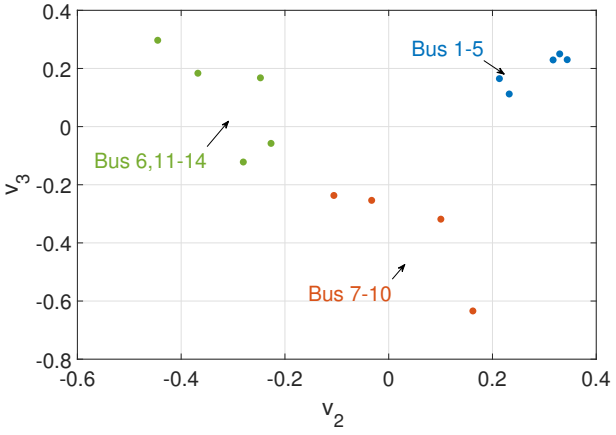

Fig. 3. New coordinate system based on eigenvectors $\boldsymbol{v}_2$, $\boldsymbol{v}_3$

Based on one eigenvector, we are able to separate a connected graph into two subareas. To generate three partitions, we need two eigenvectors. In this case, we use the 2nd and 3rd eigenvectors.

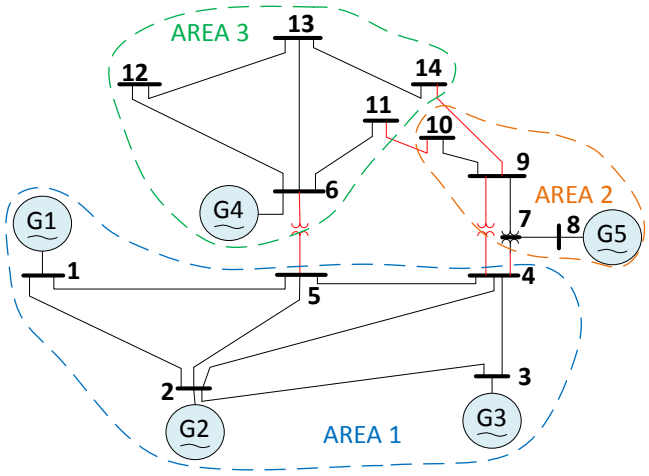

Fig. 4. Partitioning of 14-bus network

Let us take a look at the second column of $\boldsymbol{v}$. We notice that the 1st-5th, 7th and 8th elements are positive while the rest ones are negative. Thus, bus $\{1-5, 7, 8\}$ are more closely connected. Similarly, we can conclude that bus $\{1-6, 12, 13\}$ are closely connected from the third eigenvector. The first k smallest eigenvalues can supply us enough clustering information if we would like to generate a k-area partitioning. It is much easier for K-means algorithm to converge with reduced data, which is in 14×3 dimension.

The first constant eigenvector is ignored and we map each row of $\boldsymbol{v}_2$, $\boldsymbol{v}_3$ to a new coordinate system in Fig. 3. Then K-means clustering or Gaussian elimination can be applied to partitioning based on the new point set. The partition result is shown in Fig. 4 based on Fig. 3.

B. MIP Partitioning

In Ref. [5], the splitting strategy is conducted using MIP. The objective is to minimize the total load shedding under the splitting constraints, physical constraints, and connectivity constraints.

1) Objective Function: The objective function is to minimized the total load shedding. The load demand at each bus is a decision variable.

$$\min_{\mathcal{X}} \sum_{i=1}^{N_d} (D_i^{\max} - D_i) \tag{15}$$

where N_d is the number of buses with demand loads. $D_i^{\max}$ denotes the maximum of load demand at bus i, or the load demand at connected condition. D_i denotes the load demand variable at bus i. The decision variable $\mathcal{X}$ is defined as

$$\mathcal{X} = (\boldsymbol{D}^{N_d \times 1}, \quad \boldsymbol{P}^{N_g \times 1}, \quad \overline{\boldsymbol{P}}^{N_r \times 1}, \quad \boldsymbol{T}^{m \times 1}, \quad \overline{\boldsymbol{T}}^{m \times 1}, \quad \boldsymbol{\theta}^{n \times 1}, \quad \boldsymbol{x}^{n \times N_p}, \quad \boldsymbol{y}^{m \times 1})$$

where N_p, N_g and N_r refer to numbers of areas, generators and reference buses, respectively. n and m are the total numbers of buses and branches, respectively. Each variable vector is listed as follows.

- $\boldsymbol{D}^{N_d \times 1}$: The load demand vector.
- $\boldsymbol{P}^{N_g \times 1}$: The generator output power vector.
- $\overline{\boldsymbol{P}}^{N_r \times 1}$: The integer output power vector of reference buses for connectivity constraints.
- $\boldsymbol{T}^{m \times 1}$: The transmission line power vector.
- $\overline{\boldsymbol{T}}^{m \times 1}$: The integer transmission line power vector for connectivity constraints.
- $\boldsymbol{\theta}^{n \times 1}$: The voltage angle vector for all buses.
- $\boldsymbol{x}^{n \times N_p}$: $x_{i,k} = 1$ means bus i belongs to area k. Otherwise, $x_{i,k} = 0$.
- $\boldsymbol{y}^{m \times 1}$: $y_l = 1$ indicates branch l is an internal branch of one area. Otherwise, $y_l = 0$.

2) Splitting constraints:

$$\sum_{k=1}^{N_p} \boldsymbol{x}_{i,k} = 1, \quad i \in V,\ k = 1, \ldots, N_p \tag{16}$$

$\boldsymbol{x}_{i,k} = 1$, If the generator on bus i is assigned to area k. (17)

$$y_l = \sum_{k=1}^{N_p} x_{f(l),k} \cdot x_{t(l),k}, \quad \forall l \in E \tag{18}$$

Denote V and E as the bus set and branch set. $\mathcal{G}$ is the generator set. (16) is to assign each bus to an area. (17) is to decide how to distribute the generator buses. e.g., we can add $x_{2,1} = 1$ as an initial constraint to assign bus 2 to area 1. The relationship between y_l and $x_{i,k}$ is written as (18). Take branch $l_{1,2}$ and branch $l_{4,7}$ in Fig. 4 for example. $y_{l_{1,2}} = 1$ since bus 1 and bus 2 belong to the same area while $y_{l_{4,7}} = 0$ since bus 4 and bus 7 belong to different areas.

3) Power system physical constraints: This part is essentially the constraints of DC optimal power flow (OPF). The difference is that there are several disconnected subsystems. We need to describe DC OPF for each subsystems. For each subsystem, a reference bus should be identified. Also a branch l is an internal branch if $y_l = 1$, otherwise $y_l = 0$. To accommodate that last condition, big-M technique is employed.

$$\sum_{f(l)\to t(l)} T_l - \sum_{t(l)\to f(l)} T_l = P_{f(l)} - D_{f(l)},\ \forall (f(l), t(l)) \in E(l) \tag{19}$$

$$\begin{cases} \theta_i = 0, i \in \mathcal{R} \\ -\pi \le \theta_i \le \pi, i \notin \mathcal{R} \end{cases} \tag{20}$$

$$-T_l^{\max} y_l \le T_l \le T_l^{\max} y_l, \quad l \in E \tag{21}$$

$$-M(1 - y_l) \le T_l - b_l(\theta_f - \theta_t) \le M(1 - y_l), \quad l \in E \tag{22}$$

$$P_i^{\min} \le P_i \le P_i^{\max}, \quad i \in \mathcal{G} \tag{23}$$

$$D_i^{\min} \le D_i \le D_i^{\max}, \quad i \in \mathcal{L} \tag{24}$$

(19) is the power balance constraint for each from bus ($f(l) \to t(l)$ is to indicate the power flow direction). In (20), we define the bounds of voltage angle: it equals to 0 if it is the reference bus, otherwise belongs to $\{-\pi, \pi\}$. $\mathcal{R}$ is the reference bus set. Here, each area has one reference bus. (21),(22) are the transmission line capacity constraint, where M is a large constant number, b_l is the susceptance of branch l, and θ is the voltage angle. Those constraints mean that for boundary branches ($y_l = 0$), we don't need to enforce line flow equality constraints and limit constraints. When $y_l = 1$, the line limit constraints are enforced. Otherwise, these constraints are relaxed. (23) and (24) is to define the upper and lower bounds of power generations and load demands. $\mathcal{L}$ denotes the load set.

We prefer the generator buses as reference buses ($\mathcal{R}$). In the 14-bus system, we can perform Kron reduction [10] on Y bus matrix to get a Y bus matrix with the dimension of 5×5 for generators. Then we apply the same spectral clustering algorithm on generator grouping, which is similar to the spectral partitioning approach in Section II. Thus, we can select one generator bus as the reference bus in each area. Here, bus 1, 6 and 8 are selected as the reference bus for each area, respectively.

4) Subgraph connectivity constraints: Constrains (25)-(27) are to guarantee the connectivity of each area.

$$\sum_{t(l)\to f(l)} \overline{T_l} - \sum_{f(l)\to t(l)} \overline{T_l} + \overline{P}_{f(l)} - 1 = 0,\ \forall (f(l), t(l)) \in E(l) \tag{25}$$

$$-M y_l \le \overline{T_l} \le M y_l, \quad l \in E \tag{26}$$

$$\begin{cases} \overline{P_r} \ge 2, & r \in \mathcal{R} \\ \overline{P_i} = 0, & i \notin \mathcal{R} \end{cases} \tag{27}$$

Different from the physical T_l and P, $\overline{T_l}$ and $\overline{P}$ serve as dummy variables (integers). We assume the reference bus is the power supply in an area, and each bus has a unit load demand, which is 1. Notice that the dummy power flow equality constraint (25) is for every bus. $\overline{P}_{f(l)}$ is required to be 0 if it is not a reference bus with a power supply in (27). And $\overline{P}_{f(l)}$ decides the size of subgraph. Similar to (21), (26) is to cut off boundary branches.

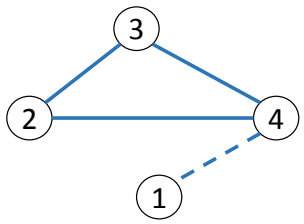

Fig. 5. Subgraph connectivity example

Let us take the subgraph in Fig. 5 for example. We assign bus 1 as the reference bus. In the first scenario, we assume the branch $l_{1,4}$ is disconnected. Then the equation (25) for each bus can be listed as follows.

$$\text{Bus 1:} \qquad \overline{P}_1 - 1 = 0 \tag{28a}$$

$$\text{Bus 2:} \ \overline{T}_{l(3,2)} + \overline{T}_{l(4,2)} + \qquad \overline{P}_2 - 1 = 0 \tag{28b}$$

$$\text{Bus 3:} \ \overline{T}_{l(2,3)} + \overline{T}_{l(4,3)} + \qquad \overline{P}_3 - 1 = 0 \tag{28c}$$

$$\text{Bus 4:} \ \overline{T}_{l(2,4)} + \overline{T}_{l(3,4)} + \qquad \overline{P}_4 - 1 = 0 \tag{28d}$$

We solve (28a) to find that $\overline{P}_1 = 1$. Note $\overline{P}_2 = 0$, $\overline{P}_3 = 0$, and $\overline{P}_4 = 0$ since Buses 2, 3, 4 are not reference

buses. Further, summing up (28b) to (28d) leads to $-3 = 0$. This constraint cannot be satisfied. Therefore, this subgraph is disconnected.

In the second scenario, we assume the branch $l_{1,4}$ is connected. Then the equation (25) for each bus can be listed as follows.

$$\text{Bus 1: } \overline{T}_{l(4,1)}+ \qquad \overline{P}_1 - 1 = 0 \quad (29a)$$

$$\text{Bus 2: } \overline{T}_{l(3,2)} + \overline{T}_{l(4,2)}+ \qquad \overline{P}_2 - 1 = 0 \quad (29b)$$

$$\text{Bus 3: } \overline{T}_{l(2,3)} + \overline{T}_{l(4,3)}+ \qquad \overline{P}_3 - 1 = 0 \quad (29c)$$

$$\text{Bus 4: } \overline{T}_{l(1,4)} + \overline{T}_{l(2,4)} + \overline{T}_{l(3,4)}+ \qquad \overline{P}_4 - 1 = 0 \quad (29d)$$

Notice that $\overline{P}_1 = \overline{P}_2 = \overline{P}_3 = 0$. If equations (29a) to (29d) are satisfied and we may sum them up and find $\overline{P}_4 = 4$, which is the number of total buses in this subgraph. We also get $\overline{T}_{l(1,4)} = -\overline{T}_{l(4,1)} = 3$, $\overline{T}_{l(4,2)} = -\overline{T}_{l(2,4)} = 1$, $\overline{T}_{l(4,3)} = -\overline{T}_{l(3,4)} = 1$, and $\overline{T}_{l(2,3)} = -\overline{T}_{l(2,3)} = 0$. All constraints can be satisfied. Hence this subgraph connectivity is guaranteed.

5) 14-bus System Partition Result: The MIP partitioning on IEEE 14-bus system is achieved through Gurobi in Python. We can get the final optimal solution is 72.68 kW. Solving time is 0.09s. And the network partitioning result is same as Fig. 4. That is due to combining the physical constraints with the objective function, MIP partitioning method can consider both minimum edge cuts and tight connection inside each area.

III. Dynamic Approach

The dynamic approach is via generator slow coherency grouping algorithm [6]. It is based on interarea oscillation mode's eigenvector to identify the coherent generators.

TABLE I
14-Bus System Generators Parameters. (Impedances are in pu.)

MVA	x_1	r_a	x_d	x'_d	x''_d	
900	0.2	0	1.8	0.3	0.25	
T_{do}	T'_{do}	x_q	x'_q	x''_q	T_{qo}	T'_{qo}
8	0.03	1.7	0.55	0.24	0.4	0.05
H	D					
6.5	0					

A. Electromechanical Models

In [6], the author presented how to build the classical electromechanical model. The generator rotor angle δ can be written as:

$$\begin{aligned}\frac{H_i}{\pi f_0}\ddot{\delta}_i &= P_{mi} - P_{ei} \\ &= P_{mi} - \frac{|E_i||V_j|\sin(\delta_i - \theta_j)}{x'_{di}}\end{aligned} \quad (30)$$

where P_{mi} and P_{ei} is input mechanical power and output electrical power, respectively. $|E_i|$ is the internal voltage magnitude of generator i with a transient reactance x'_{di}. H_i is the machine inertia constant. $|V_j|$ is the terminal bus voltage of generator i. And θ_j is the j bus voltage angle, which is computed by (31).

$$|V_j| = \sqrt{V_{j,re}^2 + V_{j,im}^2}, \quad \theta_j = \tan^{-1}(\frac{V_{j,im}}{V_{j,re}}) \quad (31)$$

The dynamic model can be formed as follows.

$$\boldsymbol{M}\ddot{\boldsymbol{\delta}} = f(\boldsymbol{\delta},\ \boldsymbol{V}) \quad (32)$$

$$0 = g(\boldsymbol{\delta},\ \boldsymbol{V}) \quad (33)$$

where (32) is in brief of (30). (33) is power flow equations at each load bus. $\boldsymbol{\delta}$ is the rotor angle vector. $\boldsymbol{V}$ is the $2n$-vector of the real and imaginary parts of bus voltages.

We can get deviations of (32) and (33) respecting to an initial power flow equilibrium $(\delta_0,\ V_0)$ to obtain a linear model:

$$\boldsymbol{M}\Delta\ddot{\delta} = \left.\frac{\partial f(\delta,V)}{\partial \delta}\right|_{\delta_0,V_0} + \left.\frac{\partial f(\delta,V)}{\partial V}\right|_{\delta_0,V_0} = \boldsymbol{K}_1\Delta\boldsymbol{\delta} + \boldsymbol{K}_2\Delta\boldsymbol{V} \quad (34a)$$

$$0 = \left.\frac{\partial g(\delta,V)}{\partial \delta}\right|_{\delta_0,V_0} + \left.\frac{\partial g(\delta,V)}{\partial V}\right|_{\delta_0,V_0} = \boldsymbol{K}_3\Delta\boldsymbol{\delta} + \boldsymbol{K}_4\Delta\boldsymbol{V} \quad (34b)$$

where $\boldsymbol{K}_1 \in \mathbb{R}^{N_g \times N_g}$ and $\boldsymbol{K}_2 \in \mathbb{R}^{N_g \times 2N_g}$ consist of the partial derivatives of power transfer between machines and their terminal buses. $\boldsymbol{K}_3 \in \mathbb{R}^{2N_g \times N_g}$ and $\boldsymbol{K}_4 \in \mathbb{R}^{2N_g \times 2N_g}$ are the partial derivatives of power transfer between terminal buses.

From (34b), we can have:

$$\Delta\boldsymbol{V} = -\boldsymbol{K}_4^{-1}\boldsymbol{K}_3\Delta\boldsymbol{\delta} \quad (35)$$

Substitute $\Delta\boldsymbol{V}$ by (35) in (34a). We can obtain a linearized electromechanical model.

$$\Delta\ddot{\delta} = \boldsymbol{M}^{-1}\boldsymbol{K}\Delta\delta \quad (36)$$

where $\boldsymbol{M}$ is a diagonal matrix of generator inertias. The entries of $\boldsymbol{M}$ can be derived from the left hand of (30).

$$M_{ii} = \frac{H_i}{\pi f_0}\text{MVA} \quad (37)$$

where MVA is the base power and H_i is in p.u..

B. Slow coherency identification

In this subsection, we show the clustering based on eigenvector of $\boldsymbol{M}^{-1}K$. We may rewrite the dynamic model using (36).

$$\underbrace{\begin{bmatrix}\Delta\dot{\delta}\\ \Delta\ddot{\delta}\end{bmatrix}}_{\dot{\boldsymbol{x}}} = \underbrace{\begin{bmatrix}\boldsymbol{0} & \boldsymbol{I}\\ \boldsymbol{M}^{-1}\boldsymbol{K} & \boldsymbol{0}\end{bmatrix}}_{\boldsymbol{A}}\underbrace{\begin{bmatrix}\Delta\delta\\ \Delta\dot{\delta}\end{bmatrix}}_{\boldsymbol{x}} \quad (38)$$

We may solve the characteristic equation to find the eigenvalues λ of $\boldsymbol{A}$.

$$\left|\lambda\boldsymbol{I} - \begin{bmatrix}\boldsymbol{0} & \boldsymbol{I}\\ \boldsymbol{M}^{-1}\boldsymbol{K} & \boldsymbol{0}\end{bmatrix}\right| = 0, \quad (39)$$

which is equivalent to

$$\begin{vmatrix}\boldsymbol{\lambda I} & -\boldsymbol{I}\\ -\boldsymbol{M}^{-1}\boldsymbol{K} & \boldsymbol{\lambda I}\end{vmatrix} = |\lambda^2\boldsymbol{I} - \boldsymbol{M}^{-1}\boldsymbol{K}| = 0 \quad (40)$$

From (40) we can see that λ^2 is an eigenvalues of $\boldsymbol{M}^{-1}\boldsymbol{K}$ if λ is an eigenvalue of $\boldsymbol{A}$. Hence, eigenvalues of $\boldsymbol{M}^{-1}\boldsymbol{K}$ can

reflect the features of $\boldsymbol{A}$. With this conclusion, we can have the eigenvectors of $\boldsymbol{A}$ and $\boldsymbol{M}^{-1}\boldsymbol{K}$ as (41).

$$\boldsymbol{A}\boldsymbol{v} = \lambda \boldsymbol{v} \tag{41a}$$

$$\boldsymbol{M}^{-1}\boldsymbol{K}\boldsymbol{v}_m = \lambda^2 \boldsymbol{v}_m \tag{41b}$$

Assume $\boldsymbol{v} = [\boldsymbol{v}_1 \quad \boldsymbol{v}_2]^T$, where $\boldsymbol{v}_1,\ \boldsymbol{v}_2 \in \mathbb{R}^{N_g \times 1}$. N_g is the number of generators. Then rewrite the equation (41a) as follows.

$$\begin{bmatrix} \boldsymbol{0} & \boldsymbol{I} \\ \boldsymbol{M}^{-1}\boldsymbol{K} & \boldsymbol{0} \end{bmatrix} \begin{bmatrix} \boldsymbol{v}_1 \\ \boldsymbol{v}_2 \end{bmatrix} = \begin{bmatrix} \boldsymbol{v}_2 \\ \boldsymbol{M}^{-1}\boldsymbol{K}\boldsymbol{v}_1 \end{bmatrix} = \lambda \begin{bmatrix} \boldsymbol{v}_1 \\ \boldsymbol{v}_2 \end{bmatrix} \tag{42}$$

Hence, we get

$$\boldsymbol{v}_2 = \lambda \boldsymbol{v}_1 \tag{43a}$$

$$\boldsymbol{M}^{-1}\boldsymbol{K}\boldsymbol{v}_1 = \lambda \boldsymbol{v}_2 \tag{43b}$$

Comparing with (41b), we find

$$\boldsymbol{v}_1 = \boldsymbol{v}_m \tag{44a}$$

$$\boldsymbol{v}_2 = \lambda \boldsymbol{v}_m \tag{44b}$$

Therefore, the eigenvectors $\boldsymbol{v}_m$ of $\boldsymbol{M}^{-1}\boldsymbol{K}$ can be used for clustering. Also the eigenvalue of $\boldsymbol{M}^{-1}\boldsymbol{K}$ is the square of $\boldsymbol{A}$'s eigenvalue.

IEEE 14-bus 5-generator network (Fig. 4) is used to test slow-coherency grouping algorithm. All the generators share the same parameters, which are shown in TABLE I. We will split generators into three groups. Implement the system bus, line and generator data to Coherency Toolbox of PST [11], we can get the matrix $\boldsymbol{M}^{-1}K$ by `svm_em` command.

$$\boldsymbol{M}^{-1}K = \begin{bmatrix} -14.3974 & 13.3881 & 4.5101 & 3.8267 & 4.2270 \\ 7.3138 & -6.8699 & -2.2443 & -1.9210 & -2.1331 \\ 4.5899 & -4.2043 & -1.5305 & -1.2073 & -1.3413 \\ 2.6820 & -2.4631 & -0.8259 & -0.7775 & -0.7711 \\ 1.3635 & -1.2528 & -0.4181 & -0.3455 & -0.4438 \end{bmatrix}$$

The eigenvalues of $\boldsymbol{M}^{-1}\boldsymbol{K}$ matrix are as follows.

$$\boldsymbol{\lambda}_m = [0.0011 \quad -0.0516 \quad -0.0805 \quad -0.1348 \quad -23.7533]^T. \tag{45}$$

The corresponding eigenvectors are:

$$\boldsymbol{v}_m = \begin{bmatrix} -0.6852 & -0.0962 & 0.0769 & -0.1549 & 0.8441 \\ -0.4113 & -0.2804 & 0.1721 & -0.4803 & -0.4293 \\ -0.3477 & -0.3318 & 0.2562 & 0.8584 & -0.2689 \\ -0.3511 & 0.0225 & -0.9100 & 0.0925 & -0.1569 \\ -0.3423 & 0.8953 & 0.2658 & -0.0009 & -0.0796 \end{bmatrix}$$

The eigenvectors indicates the relative motions of the generators, i.e., sharing the same sign in $\boldsymbol{v}_{m1}$ represent the system mode in which all generators move together in the same direction and proportion. $\boldsymbol{v}_{m2}$ is to indicate the $\lambda_2 = \sqrt{\lambda_{m2}} = \sqrt{-0.0516} = \pm j0.2272$ rad/s interarea mode in which generator 5 oscillates against the rests. And $\boldsymbol{v}_{m3}$ is to indicate the $\lambda_3 = \sqrt{\lambda_{m3}} = \sqrt{-0.0805} = \pm j0.2837$ rad/s interarea mode in which generator 4 oscillates against the rests. $\boldsymbol{v}_{m4}$ and $\boldsymbol{v}_{m5}$ are for Area 1's local modes. Gaussian elimination can be performed on the first three eigenvectors to identify three generator groups numerically. The generator grouping result is presented in Fig. 6. We can see it matches the generator grouping in Fig. 4 as well. Since we assume all generators sharing the same feature, only the admittance matrix has the effect on dynamic model's inter-area modes. And both spectral clustering and MIP partitioning depend on admittance to identify the tightly connected buses.

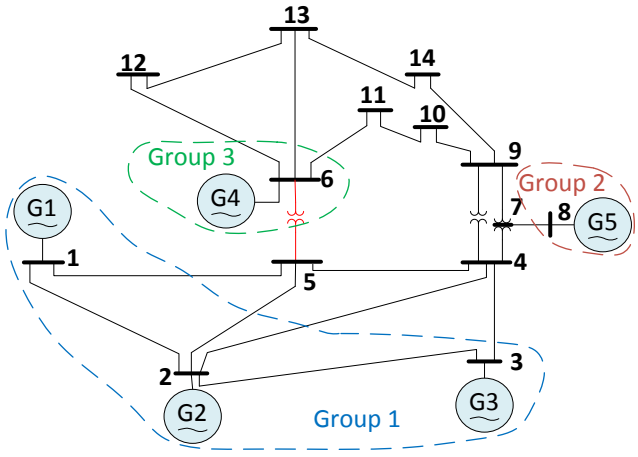

Fig. 6. IEEE 14-bus system generators grouping

IV. Conclusion

In this paper, we give a detailed understanding of power system partitioning via static and dynamic aspects. We found that a similar result can be carried out via spectral clustering and MIP partitioning due to their common motivation. Also, the similarity of spectral clustering and slow coherency is identified via the studies on IEEE 14-bus system. The admittance matrix has a direct effect on eigenvector-based clustering. It provides insight into the relationship between power system static structure and generator dynamic model.

References

[1] X. Xu, F. Xue, S. Lu, H. Zhu, L. Jiang, and B. Han, "Structural and hierarchical partitioning of virtual microgrids in power distribution network," *IEEE Systems Journal*, 2018.

[2] J. Guo, G. Hug, and O. K. Tonguz, "Intelligent partitioning in distributed optimization of electric power systems," *IEEE Transactions on Smart Grid*, vol. 7, no. 3, pp. 1249–1258, 2016.

[3] ——, "A case for nonconvex distributed optimization in large-scale power systems," *IEEE Transactions on Power Systems*, vol. 32, no. 5, pp. 3842–3851, 2017.

[4] U. Von Luxburg, "A tutorial on spectral clustering," *Statistics and computing*, vol. 17, no. 4, pp. 395–416, 2007.

[5] T. Ding, K. Sun, C. Huang, Z. Bie, and F. Li, "Mixed-integer linear programming-based splitting strategies for power system islanding operation considering network connectivity," *IEEE Systems Journal*, 2015.

[6] J. H. Chow, *Power system coherency and model reduction*. Springer, 2013.

[7] L. Fan, "Interarea oscillations revisited," *IEEE Transactions on Power Systems*, vol. 32, no. 2, pp. 1585–1586, 2017.

[8] T. Ishizaki, A. Chakrabortty, and J.-I. Imura, "Graph-theoretic analysis of power systems," *Proceedings of the IEEE*, vol. 106, no. 5, pp. 931–952, 2018.

[9] L. Guo, C. Zhao, and S. H. Low, "Graph laplacian spectrum and primary frequency regulation," *arXiv preprint arXiv:1803.03905*, 2018.

[10] G. Kron, *Tensor analysis of networks*. J. Wiley & Sons, 1939.

[11] J. H. Chow and K. W. Cheung, "A toolbox for power system dynamics and control engineering education and research," *IEEE transactions on Power Systems*, vol. 7, no. 4, pp. 1559–1564, 1992.